

Online Appendix: “Multidimensional Auctions of Contracts: An Empirical Analysis”

Yunmi Kong

Isabelle Perrigne

Quang Vuong

A Proofs

Verification of Assumption A1 for Option Value: In view of Table 2, we only need to show that $V_a(a, \theta_1, \theta_2)$ is decreasing in θ_1 and increasing in θ_2 . Let $R \equiv (1 - a)p\theta_1$. By the chain rule and product rule of derivatives, we have for $k = 1, 2$

$$\frac{\partial}{\partial \theta_k} V_a(a; \theta_1, \theta_2) = \frac{\partial}{\partial \theta_k} \left(\frac{\partial V}{\partial R} \frac{\partial R}{\partial a} \right) = \frac{\partial}{\partial \theta_k} \left(\frac{\partial V}{\partial R} \right) \frac{\partial R}{\partial a} + \frac{\partial}{\partial \theta_k} \left(\frac{\partial R}{\partial a} \right) \frac{\partial V}{\partial R}.$$

It is well known from the option pricing literature (see Hull (2017)) that $\partial V / \partial R = e^{-rt} \Phi(x)$. So using this and the definition of x in (2) leads to

$$\begin{aligned} \frac{\partial}{\partial \theta_1} \left(\frac{\partial V}{\partial R} \right) &= e^{-rt} \phi(x) \frac{\partial x}{\partial \theta_1} = e^{-rt} \phi(x) \frac{1}{\theta_1 \sigma \sqrt{t}}, \\ \frac{\partial}{\partial \theta_2} \left(\frac{\partial V}{\partial R} \right) &= e^{-rt} \phi(x) \frac{\partial x}{\partial \theta_2} = e^{-rt} \phi(x) \frac{1}{-\theta_2 \sigma \sqrt{t}}. \end{aligned}$$

Meanwhile, $\partial R / \partial a = -p\theta_1$, so $\partial(\partial R / \partial a) / \partial \theta_1 = -p$ and $\partial(\partial R / \partial a) / \partial \theta_2 = 0$. Plugging these into the above first equation, we have

$$\begin{aligned} \frac{\partial}{\partial \theta_1} V_a(a; \theta_1, \theta_2) &= -e^{-rt} \phi(x) \frac{1}{\theta_1 \sigma \sqrt{t}} p \theta_1 - p e^{-rt} \Phi(x) < 0, \\ \frac{\partial}{\partial \theta_2} V_a(a; \theta_1, \theta_2) &= e^{-rt} \phi(x) \frac{1}{\theta_2 \sigma \sqrt{t}} p \theta_1 + 0 > 0. \end{aligned}$$

Verification of Necessary Identification Condition for Option Value: A necessary condition for identification is that the system $V_a(a; \theta_1, \theta_2) = Y_1$ and $V(a; \theta_1, \theta_2) = Y_2$ has at most one solution in (θ_1, θ_2) given (a, Y_1, Y_2) . Indeed, if this was not the case, then (8)-(9) would have more than one solution in (θ_1, θ_2) . We now prove that the option value in (1)-(2) satisfies this condition. Since (2) is a monotonic function of the ratio θ_1 / θ_2 , we use a change of variables to solve (8)-(9) for θ_1 and x instead of θ_1 and θ_2 . First, we use (8) to express θ_1 in terms of x . Second, we plug this expression for θ_1 into (9), yielding an equation with one unknown x . Third, we show that there cannot be more than one solution x to this equation. Finally, we give closed-form expressions for θ_1 and θ_2 as functions of the solution x .

First, we define $R \equiv (1 - a)p\theta_1$. We have $V_a(a; \theta_1, \theta_2) = (\partial V / \partial R)(\partial R / \partial a) = -e^{-rt} p \theta_1 \Phi(x)$ using $\partial V / \partial R = e^{-rt} \Phi(x)$. See Hull (2017). Substituting this into the left-hand side of (8) leads to $-e^{-rt} p \theta_1 \Phi(x) = Y_1$. Hence, $\theta_1 = -Y_1 / [e^{-rt} p \Phi(x)] = C_1 / \Phi(x)$, where $C_1 = -Y_1 / [e^{-rt} p] > 0$ is a known constant.

Second, plugging this expression for θ_1 in (1) gives

$$\begin{aligned}
V(a; \theta_1, \theta_2) &= e^{-rt}(1-a)p\theta_1 \left[\Phi(x) - \theta_2 \Phi(x - \sigma\sqrt{t}) / ((1-a)p\theta_1) \right] \\
&= e^{-rt}(1-a)p(C_1/\Phi(x)) \left[\Phi(x) - \theta_2 \Phi(x - \sigma\sqrt{t}) / ((1-a)p\theta_1) \right] \\
&= e^{-rt}(1-a)pC_1 \left[1 - \theta_2 \Phi(x - \sigma\sqrt{t}) / ((1-a)p\theta_1\Phi(x)) \right] \\
&= e^{-rt}(1-a)pC_1 \left[1 - e^{-\sigma\sqrt{t}x} e^{\sigma^2 t/2} \Phi(x - \sigma\sqrt{t}) / \Phi(x) \right],
\end{aligned}$$

where the last equality follows from $\theta_2 / [(1-a)p\theta_1] = \exp(-\sigma\sqrt{t}x + \sigma^2 t/2)$ by (2). Using this expression for $V(a; \theta_1, \theta_2)$ in (9) gives

$$e^{-rt}(1-a)pC_1 \left(1 - e^{-\sigma\sqrt{t}x} e^{\sigma^2 t/2} \frac{\Phi(x - \sigma\sqrt{t})}{\Phi(x)} \right) = Y_2.$$

Collecting x on the left-hand side yields

$$e^{-\sigma\sqrt{t}x} \frac{\Phi(x - \sigma\sqrt{t})}{\Phi(x)} = e^{-\sigma^2 t/2} \left(1 - \frac{Y_2}{e^{-rt}(1-a)pC_1} \right). \quad (\text{A.1})$$

Third, the right-hand side of (A.1) is known and denoted C_2 . We show that the left-hand side is strictly monotonic in x , so that there cannot be more than one value of x satisfying (A.1). Taking the derivative of the left-hand side with respect to x gives

$$\begin{aligned}
\frac{\partial}{\partial x} \left(e^{-\sigma\sqrt{t}x} \frac{\Phi(x - \sigma\sqrt{t})}{\Phi(x)} \right) &= -\sigma\sqrt{t} e^{-\sigma\sqrt{t}x} \frac{\Phi(x - \sigma\sqrt{t})}{\Phi(x)} + e^{-\sigma\sqrt{t}x} \left(\frac{\phi(x - \sigma\sqrt{t})\Phi(x) - \Phi(x - \sigma\sqrt{t})\phi(x)}{\Phi(x)^2} \right) \\
&= \left(e^{-\sigma\sqrt{t}x} / \Phi(x) \right) \left(-\sigma\sqrt{t}\Phi(x - \sigma\sqrt{t}) + \phi(x - \sigma\sqrt{t}) - \frac{\phi(x)}{\Phi(x)}\Phi(x - \sigma\sqrt{t}) \right) \\
&= \left(e^{-\sigma\sqrt{t}x} \phi(x - \sigma\sqrt{t}) / \Phi(x) \right) \left(-\sigma\sqrt{t} \frac{\Phi(x - \sigma\sqrt{t})}{\phi(x - \sigma\sqrt{t})} + 1 - \frac{\phi(x)}{\Phi(x)} \frac{\Phi(x - \sigma\sqrt{t})}{\phi(x - \sigma\sqrt{t})} \right) \\
&= \left(e^{-\sigma\sqrt{t}x} \phi(x - \sigma\sqrt{t}) / \Phi(x) \right) \left(1 - \frac{\Phi(x - \sigma\sqrt{t})}{\phi(x - \sigma\sqrt{t})} \left(\sigma\sqrt{t} + \frac{\phi(x)}{\Phi(x)} \right) \right).
\end{aligned}$$

But $h'(x) > -1$, where $h(x) \equiv \frac{\phi(x)}{\Phi(x)}$.¹ Thus

$$\sigma\sqrt{t} + \frac{\phi(x)}{\Phi(x)} > \frac{\phi(x - \sigma\sqrt{t})}{\Phi(x - \sigma\sqrt{t})} \Rightarrow 1 - \frac{\Phi(x - \sigma\sqrt{t})}{\phi(x - \sigma\sqrt{t})} \left(\sigma\sqrt{t} + \frac{\phi(x)}{\Phi(x)} \right) < 0,$$

for any value of $\sigma\sqrt{t}$. Thus from the above derivative, it follows that $\frac{\partial}{\partial x} \left(e^{-\sigma\sqrt{t}x} \frac{\Phi(x - \sigma\sqrt{t})}{\Phi(x)} \right) < 0$, showing that the left-hand side of (A.1) is strictly decreasing in x . Thus, there is at most one solution in x to (A.1), which can be obtained numerically. Finally, as functions of the solution x , $\theta_1 = P_a(a, b|a, b, n) / (P_b(a, b|a, b, n)e^{-rt}p\Phi(x))$ and $\theta_2 = (1-a)p\theta_1 \exp(-\sigma\sqrt{t}x + \sigma^2 t/2)$.

¹To prove this, we adapt Sampford (1953)'s proof about the derivative of $\frac{\phi(x)}{1-\Phi(x)}$. Specifically, consider a standard normal distribution which is top-truncated at x . Its variance is $1 - \frac{x\phi(x)}{\Phi(x)} - \left(\frac{\phi(x)}{\Phi(x)} \right)^2 = 1 - xh(x) - h(x)^2 > 0$. Because $h'(x) = -xh(x) - h(x)^2$, then $h'(x) > -1$.

Proof of Proposition 1: Under assumptions A1–A4, the first-order conditions (3)-(4) become (8)-(9) as explained in the text. Thus, by the invertibility assumption A4, (8)-(9) has a unique solution in (θ_1, θ_2) given (a, b) . Hence, the private information (θ_1, θ_2) is identified for each bidder from his bid (a, b) since the RHS of (8)-(9) is identified. It follows that the $2n$ -dimensional joint distribution of types $F(\cdot, \dots, \cdot | n)$ is identified.

B Additional Details and Extensions

Bidders’ Asymmetry and Stability of Allocation Patterns: We check for asymmetry among bidders in the allocation rule and whether this rule changes over time with factors such as oil price. We observe in the data 522 different bidders’ identities. The concentration of the share of wins among bidders is very low with a Herfindhal-Hirschman index of 0.01. As is common in the empirical auction literature, we refer to bidders who participate 10 times or less as ‘fringe’ bidders. Table A1 displays the result of a probit regression to assess the effect of being a fringe bidder on the probability of winning, controlling for component-wise differences from the competing bid. The probit coefficient on the fringe bidder dummy is statistically insignificant, showing no evidence that fringe bidders are treated differently from regular bidders or face a different probability of winning conditional on bid components. The second column includes interactions with oil price to assess whether the State’s choice of winner depends on oil price. The coefficients on the oil price interactions are statistically insignificant. These probit regressions also confirm that the probability of winning is increasing in both cash payment and royalty.

Derivation of Implied Volatility: Using prices of crude oil options, we compute the implied volatility of West Texas Intermediate oil prices for each month. Specifically, we invert the Black (1976) commodity option pricing equation to back out the expected volatility implied by the price of every traded call option. We take the median of these implied volatilities in each trade month m for option maturity τ (in months) to be the implied volatility $\sigma_{\tau m}$ in month m of τ -month futures, where 1-month futures are the closest to the spot price. Implied volatilities derived from 1-month options are noisy because we observe only the month of option expiration but not the day, so that the time left to expiration may not equal an exact month. To address this noise issue, we adapt Kellogg (2014)’s method to infer the desired volatility from options with different maturities. Specifically, for each month m , we use daily realized volatilities of oil futures² in the surrounding 1-year window to estimate the fixed effects regression $\log rvol_{\tau t} = \eta_{\tau} + \delta_t + \epsilon_{\tau t}$, where $rvol_{\tau t}$ is the realized volatility of the τ -month future contract on day t , η_{τ} is a maturity fixed effect and δ_t is a day fixed effect.

²Historical crude oil futures prices were obtained from Quandl (1983-2019).

Table A1: Probit Model Probability of Winning, $n = 2$

	(1)	(2)
fringe bidder	-0.009 (0.148)	-0.011 (0.148)
log difference from competing bid's cash	2.757 (0.165)	2.966 (0.433)
difference from competing bid's royalty	20.385 (1.844)	27.327 (5.491)
log cash difference \times oil price		-0.004 (0.008)
royalty difference \times oil price		-0.133 (0.098)
constant	0.007 (0.132)	0.009 (0.132)
Pseudo R^2	0.564	0.565

Notes: Table shows probit regression of a dummy for winning the auction on the listed regressors in auctions with two bidders. For oil price, we use monthly West Texas Intermediate crude oil (WTI) prices, deflated to 2009 dollars. Observations are at the bid level. Standard errors are in parentheses.

We then infer the implied volatility σ_{1m} of 1-month futures in month m from the volatility implied by contemporary 3-month options σ_{3m} as $\sigma_{1m} = \sigma_{3m} \exp(\eta_{1m} - \eta_{3m})$.

Parameters of the Binomial Tree for Valuing American Options: In each step of a binomial tree going from node t to $t+1$, the price increases to $p_{t+1} = p_t u$ with probability q and decreases to $p_{t+1} = p_t d$ with probability $1-q$. The parameters u , d and q of the tree are chosen to match the price process of p as follows. Let Δt denote the size of each time step, which is 3/100 year given a 3-year option duration divided by 100 steps in the tree. A geometric Brownian motion with volatility σ implies that the standard deviation of the return on p during time step Δt is equal to $\sigma\sqrt{\Delta t}$. Therefore, $u = e^{\sigma\sqrt{\Delta t}}$ and $d = e^{-\sigma\sqrt{\Delta t}}$. A geometric Brownian motion with zero drift after adjusting for inflation implies that $E(p_{t+1}) = p_t$. This means $qp_t u + (1-q)p_t d = p_t$. Solving this equation for q gives $q = (1-d)/(u-d)$. See Hull (2017) for further details on binomial trees.

Bidders’ Cash Constraints: We might wonder whether bidders are cash constrained and bid higher royalties in order to pay less cash upfront. The bidding patterns we observe appear inconsistent with cash constraints being a major driver of royalty bids. As described in Section 2.1, we observe more often than not that the bidder bidding more royalty simultaneously bids more cash than competing bidders in the same auction. If higher royalty bids were from more cash constrained bidders, we would observe the opposite. This positive correlation between cash and royalty is also observed in Figure 1. To compute the correlation conditional on tract heterogeneity, we use the residuals of the two regressions of Table 3, which regress the cash and royalty components of the bids on lease covariates. The correlation coefficient between the log cash and royalty residuals is 0.32. Cash constraints do not appear to be a first-order issue in our bidding data.

Unobserved Heterogeneity: Previous empirical studies have shown that auction data might be subject to unobserved heterogeneity. One way to account for unobserved heterogeneity is to condition the value distribution on the number of bidders (as we do) to control for higher valued tracts attracting (say) more bidders. Empirically, there remains residual correlation between bids submitted to the same auction after conditioning on the covariates listed in Table 3. In two-bidder auctions, the correlation coefficient of the residuals is 0.65 for the logarithm of cash and 0.26 for royalty. These correlations can be generated by unobserved auction heterogeneity or affiliation of private information across bidders, which are difficult to distinguish from bid data. Krasnokutskaya (2011)’s deconvolution method for first-price sealed-bid auctions attributes all conditional correlation to unobserved heterogeneity. Her method relies on (i) the scale invariance property of the bidding strategy and (ii) independence of private values. In our model, the general allocation rule need not satisfy (i).³ Meanwhile, (ii) is necessary because unobserved heterogeneity is identified by assuming that all conditional correlation across bids is caused by it. Instead, we attribute the conditional correlation of each bid component across bidders to affiliation of private information while controlling for auction heterogeneity more carefully through our heatmap indices in addition to standard covariates.

Common Values: Oil lease auction data have historically been analyzed within a common value (CV) framework though private value models have been recently used for leases in areas

³The issue related to the lack of scale invariance has also been noted by Yoganarasimhan (2016) in beauty contests upon assuming independence of univariate private information across bidders. She uses discrete unobserved heterogeneity which would not be sufficient in our case. Takahashi (2018) extends Krasnokutskaya (2011)’s method to bidimensional private information by generalizing scale invariance. His result depends on a combination of assumptions including the independence of private information across and within bidders, the parametric specification of the cost function and a known scoring function in the inverse price quality ratio.

with a long antecedent of development. See e.g. Hendricks, Porter and Boudreau (1987) for the analysis of auctioned offshore leases and Kong (2020, 2021) for auctioned leases in the Permian Basin. We discuss a pure CV model with multidimensional private information.⁴ In our setting with option values, let (Q, C) denote the unknown common components, which represent the quantity of oil and production cost, respectively. Bidder i 's private information $(\theta_{1i}, \theta_{2i})$ are now interpreted as signals. The $2(n + 1)$ -vector $(Q, C, \theta_{11}, \theta_{21}, \dots, \theta_{1n}, \theta_{2n})$ is distributed as $F(\cdot, \dots, \cdot | n)$ which is affiliated. The contract value becomes $V(a_i; Q, C)$, which is common to all bidders up to their royalty bids a_i . For a bid pair (a_i, b_i) , let $W(a_i, b_i)$ be an indicator for winning and let $v(a_i, b_i; \theta_{1i}, \theta_{2i}, n) \equiv E[V(a_i; Q, C) | W(a_i, b_i) = 1, \theta_{1i}, \theta_{2i}, n]$ denote bidder i 's expected value conditional on winning. Bidder i 's expected profit from the auction is $[v(a_i, b_i; \theta_{1i}, \theta_{2i}, n) - b_i]P(a_i, b_i | \theta_{1i}, \theta_{2i}, n)$. Maximizing this expected profit with respect to (a_i, b_i) , rearranging the first-order conditions and omitting the subscript i give

$$\begin{aligned} v_a(a, b; \theta_1, \theta_2, n) - \frac{P_a(a, b | \theta_1, \theta_2, n)}{P_b(a, b | \theta_1, \theta_2, n)} v_b(a, b; \theta_1, \theta_2, n) &= -\frac{P_a(a, b | \theta_1, \theta_2, n)}{P_b(a, b | \theta_1, \theta_2, n)}, \\ v(a, b; \theta_1, \theta_2, n) + \frac{P(a, b | \theta_1, \theta_2, n)}{P_b(a, b | \theta_1, \theta_2, n)} v_b(a, b; \theta_1, \theta_2, n) &= b + \frac{P(a, b | \theta_1, \theta_2, n)}{P_b(a, b | \theta_1, \theta_2, n)}. \end{aligned}$$

The right-hand sides are identical to those in (3)-(4), whereas the left-hand sides are more complicated. In particular, one can show that the left-hand side of the second equation reduces to the standard pivotal value $E[V(a_o; Q, C) | \max_{j \neq i} b_j = b_i, \theta_i, n]$ in a first-price sealed-bid auction with fixed royalty a_o and one-dimensional private information θ_i . Our identification argument and estimation recover the left-hand sides since the right-hand sides are observed or estimable. When it comes to characterizing $v(a, b; \theta_1, \theta_2, n)$ and identifying the latent distribution $F(\cdot, \dots, \cdot | n)$ from bids, there are new difficulties arising from (i) characterization of the winner's curse under multidimensional private information and multivariate bids, (ii) the dependence of $v(a, b; \theta_1, \theta_2, n)$ on the endogenous royalty bid a as well as b and (iii) the nonstandard nature of the allocation rule. The standard common value model of first-price sealed-bid auctions with univariate private information is identified from bids with the help of, e.g., functional form restrictions or exclusion restrictions involving bidders' asymmetry. See Perrigne and Vuong (2021) for a recent survey. We doubt that the existing approaches would resolve the difficulties above. The study of such a model with multivariate bids, multidimensional private information and a general allocation rule is left for future research.

⁴More generally, we could develop an interdependent value model with multidimensional private information. For simplicity and concreteness, we consider the special case of a pure CV model.

Table A2: Decomposing the Revenue Comparison

in \$ per acre	Total	Cash	Royalty
LA cash-royalty auction	2564	882	1682
Keep LA bids but apply fixed-royalty allocation	2589	890	1700
Fixed-royalty auction (23%)	2666	994	1672

Notes: The first, second, and third columns display ex ante expected total government revenue, cash revenue, and royalty revenue in dollars per acre, respectively. Dollar amounts are in 2009 dollars. The first row is based on bids observed in the Louisiana cash royalty auction. The second row uses the same bids as the first row but counterfactually applies the allocation of a fixed royalty auction with 23% royalty. The third row counterfactually simulates a fixed royalty auction with 23% royalty.

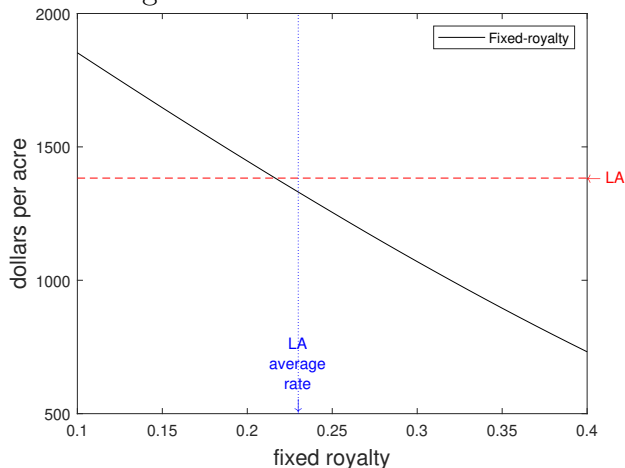
C Supplement to Sections 5.1 and 5.3

Allocative Performance: Beyond revenue, Figure A4 assesses the allocative performance of fixed-royalty auctions. We exploit the bidder’s estimated types to check whether the state allocation generates the highest ex ante expected revenue. The solid curve gives the proportion of fixed-royalty auctions that are revenue efficient. This proportion ranges from 97% to 100% as A varies. Allocative inefficiency arises because royalties are levied on revenues and not profits thereby asymmetrically affecting bidders’ and government’s payoffs. From the dashed line, we see that Louisiana does not perform as well with about 6% of auctions in which allocation is not revenue optimal. As discussed before, royalties are less costly for weak firms and serve as a ‘cheaper’ currency with which to bid, so these firms win more often than when royalty is fixed.

To quantify the misallocation issue, the second row of Table A2 takes bids from the Louisiana auction but counterfactually applies the same allocation as the 23% fixed-royalty auction, i.e., each lease is awarded to the bidder who would have won the fixed-royalty auction. Therefore, the second row quantifies the effect of changes in allocation separately from the effect of changes in bids. For comparison, the first and third rows present revenues from the Louisiana auction and the 23% fixed-royalty auction, respectively. The total revenue column shows that about one fourth of the revenue gap is due to differences in allocation, the rest arising from differences in bids. The second and third rows show that, holding allocation constant, cash-royalty bidding still causes a drop in cash revenue that is not recouped in royalty revenue.

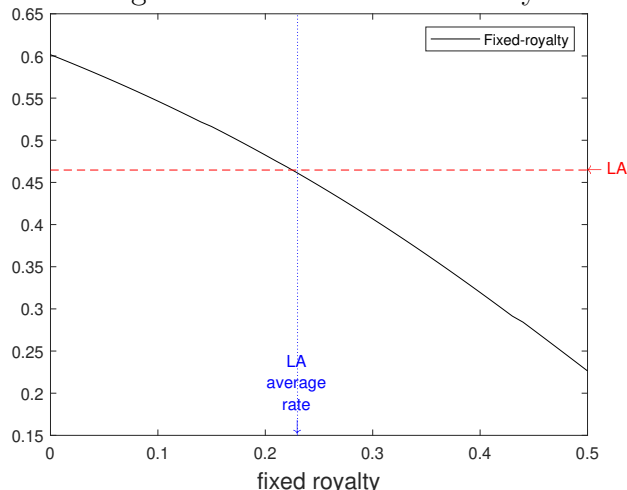
The figures below provide additional details on the counterfactual results.

Figure A1: Information Rents



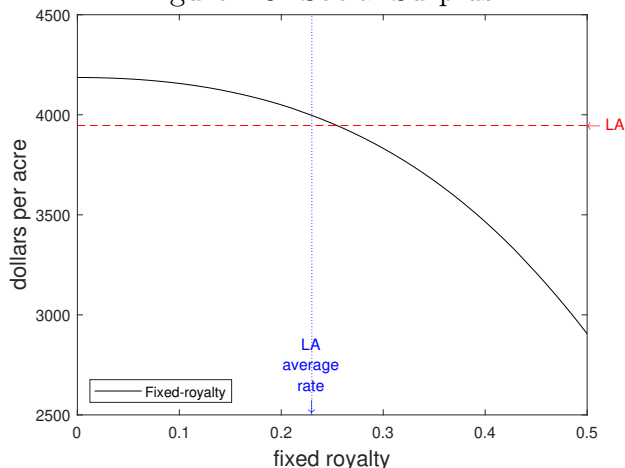
Notes: Solid line displays winning bidders' information rents from counterfactual simulations of fixed-royalty auctions, as a function of the fixed royalty rate displayed on the x -axis. For comparison, the dashed horizontal line marks information rents computed from observed bids in the Louisiana cash-royalty auction, and the vertical dotted line marks the average observed royalty rate resulting from that auction, 23%.

Figure A2: Exercise Probability



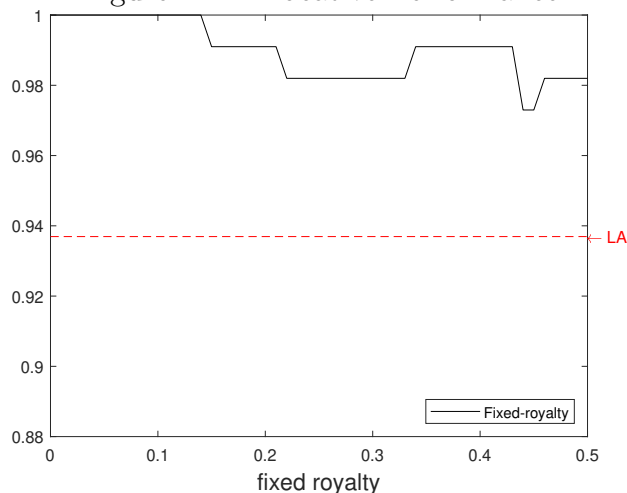
Notes: Solid line displays ex ante expected probability of lease development in counterfactual simulations of fixed-royalty auctions, as a function of the fixed royalty rate displayed on the x -axis. For comparison, the dashed horizontal line marks the analogous exercise probability computed from observed bids in the Louisiana cash-royalty auction, and the vertical dotted line marks the average observed royalty rate resulting from that auction, 23%.

Figure A3: Social Surplus



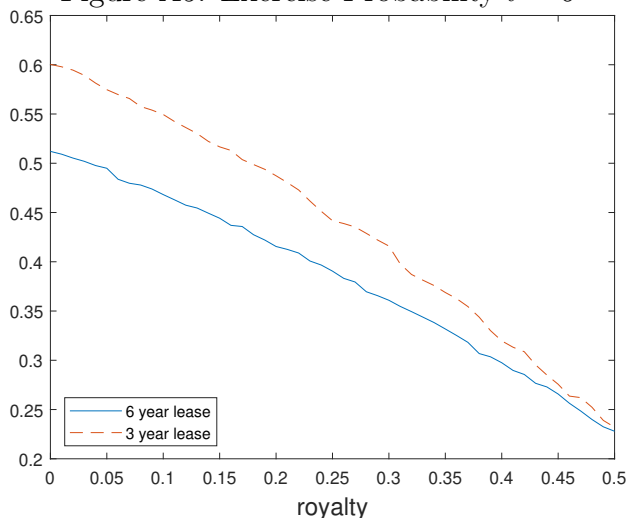
Notes: Solid line displays social surplus in counterfactual simulations of fixed-royalty auctions, as a function of the fixed royalty rate displayed on the x -axis. For comparison, the dashed horizontal line marks social surplus computed from observed bids in the Louisiana cash-royalty auction, and the vertical dotted line marks the average observed royalty rate resulting from that auction, 23%.

Figure A4: Allocative Performance



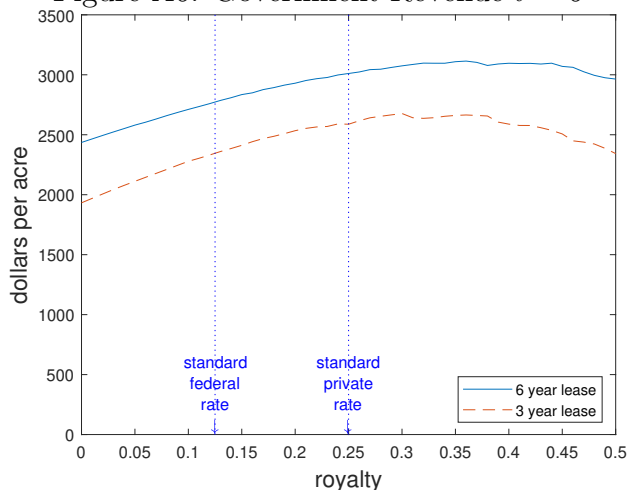
Notes: The solid line displays the proportion of fixed-royalty auctions that allocate the lease to the ex ante revenue-maximizing bidder according to counterfactual simulations, as a function of the fixed royalty rate displayed on the x -axis. For comparison, the dashed horizontal line marks the analogous proportion in the Louisiana cash-royalty auction.

Figure A5: Exercise Probability $t = 6$



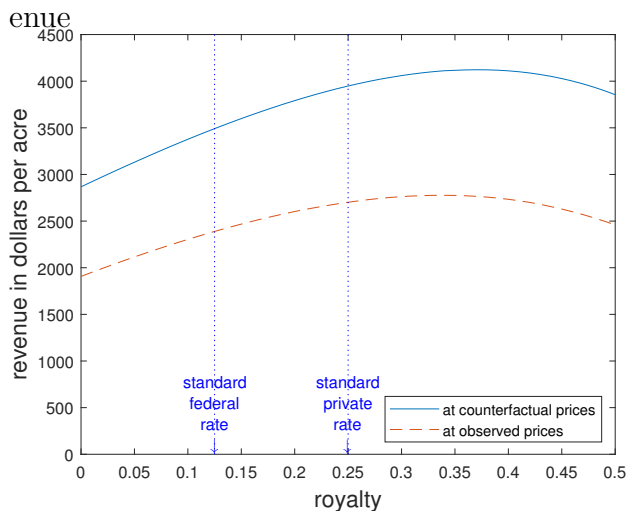
Notes: Figure displays ex ante expected probability of lease development in counterfactual simulations of fixed-royalty auctions, as a function of the fixed royalty rate displayed on the x -axis. The solid line is for a 6-year lease and the dashed line is for a 3-year lease. Leases are modeled as American options.

Figure A6: Government Revenue $t = 6$



Notes: Figure displays ex ante expected total government revenue in counterfactual simulations of fixed-royalty auctions, as a function of the fixed royalty rate displayed on the x -axis. The solid line is for a 6-year lease and the dashed line is for a 3-year lease. Leases are modeled as American options.

Figure A7: Oil Price and Government Revenue



Notes: Figure displays ex ante expected total government revenue in counterfactual simulations of fixed-royalty auctions, as a function of the fixed royalty rate displayed on the x -axis. The solid line is at oil prices 20% higher than observed, while the dashed line is at observed oil prices.

D Robustness Analysis using American Options

In this section, we repeat all the counterfactual analyses of Section 5 using American option estimates and valuations. We present the results in tables and figures corresponding to the ones shown for the European option.

Table A3: Decomposing the Revenue Comparison

in \$ per acre	Total	Cash	Royalty
LA cash-royalty auction	2444	882	1562
Keep LA bids but apply fixed-royalty allocation	2468	890	1579
Fixed-royalty auction (23%)	2569	992	1577

Notes: The first, second, and third columns display ex ante expected total government revenue, cash revenue, and royalty revenue in dollars per acre, respectively. Dollar amounts are in 2009 dollars. The first row is based on bids observed in the Louisiana cash royalty auction. The second row uses the same bids as the first row but counterfactually applies the allocation of a fixed royalty auction with 23% royalty. The third row counterfactually simulates a fixed royalty auction with 23% royalty.

Table A4: Details of Quasi-Linear Scoring Auctions

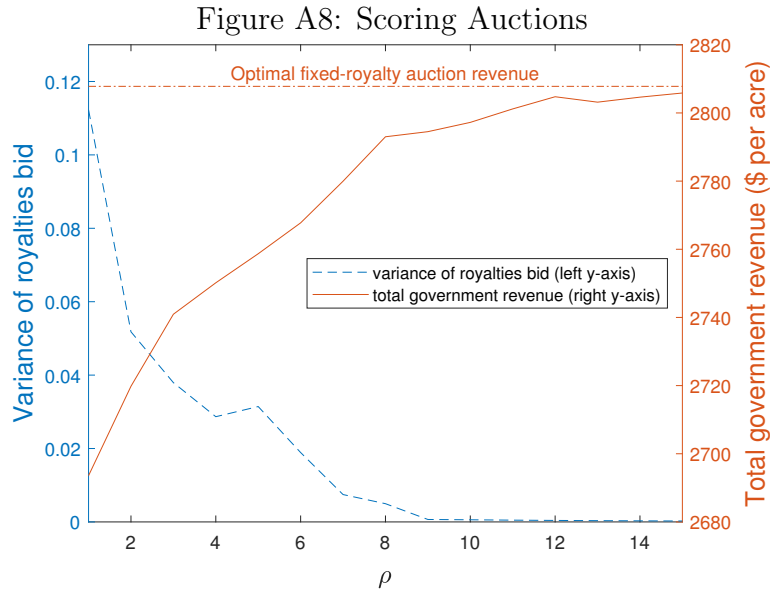
ρ	1	2	3	4	5	6	7	8	9	10
$E[(b - \underline{b}) / (s - \underline{s})]$	0.53	0.43	0.41	0.44	0.45	0.49	0.49	0.47	0.47	0.48
mean royalty bid	0.36	0.30	0.31	0.30	0.31	0.29	0.29	0.31	0.30	0.31
median royalty bid	0.20	0.23	0.25	0.26	0.27	0.27	0.28	0.31	0.30	0.31

Notes: We counterfactually simulate second-score auctions with quasi-linear scoring rules of the form $S(a, b) = b - p(\omega/a^\rho)$, where a and b are the royalty and cash components of the bid, respectively, p is the oil price, ω is a revenue-maximizing weight, and ρ determines the curvature of the scoring function. Table columns from left to right show auction outcomes associated with $\rho = 1, 2, \dots, 10$. The first row shows the expected portion of the score that is due to the cash payment b , where \underline{b} and \underline{s} are the minimum of cash and score values, respectively.

Table A5: Fixed-Royalty versus Scoring Auctions

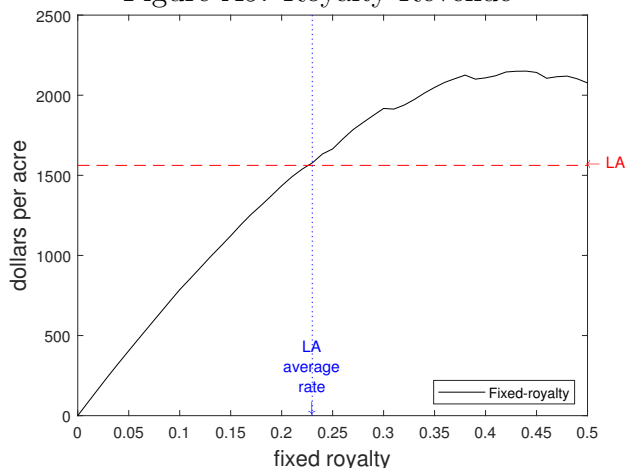
	Fixed-royalty auction	Scoring auction, $\rho = 1$
Mean royalty	30%	36%
Median royalty	30%	20%
Total government revenue	\$2,808	\$2,694
Royalty revenue	\$1,913	\$1,137
Cash revenue	\$894	\$1,557
Firm information rents	\$922	\$1,283
Same allocation as fixed-royalty	–	0.97
Pr(option exercise)	0.42	0.45
Social surplus	\$3,730	\$3,977

Notes: Table presents outcomes associated with counterfactual simulations of a second-price fixed-royalty auction in the first column, with revenue-maximizing fixed royalty of 30%, and a second-score scoring auction in the second column, which uses a quasi-linear scoring rule $S(a, b) = b - p(\omega/a^\rho)$ with curvature $\rho = 1$ and revenue-maximizing weight ω . Dollars are expressed in 2009 dollars and per acre.



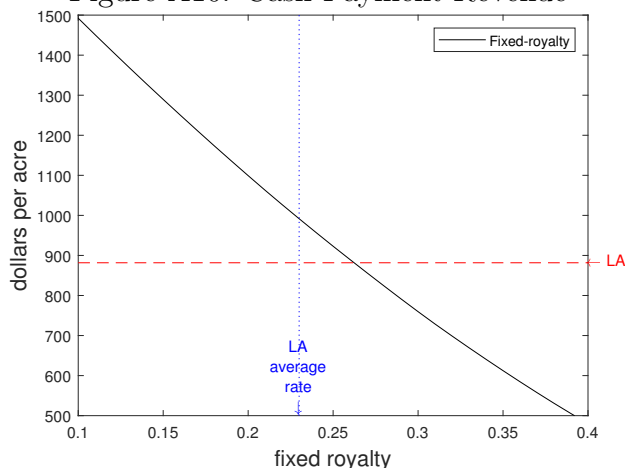
Notes: The solid line and dashed line plot simulated outcomes of a second-score scoring auction with quasi-linear scoring rule $S(a, b) = b - p(\omega/a^\rho)$, as a function of curvature parameter ρ . Given each ρ , a revenue-maximizing weight ω is used. The dashed line is to be read by the left y -axis, and the solid line is to be read by the right y -axis. For comparison, the dash-dot horizontal line to be read by the right y -axis marks simulated revenue from a second-price fixed-royalty auction with revenue-maximizing fixed royalty (30%).

Figure A9: Royalty Revenue



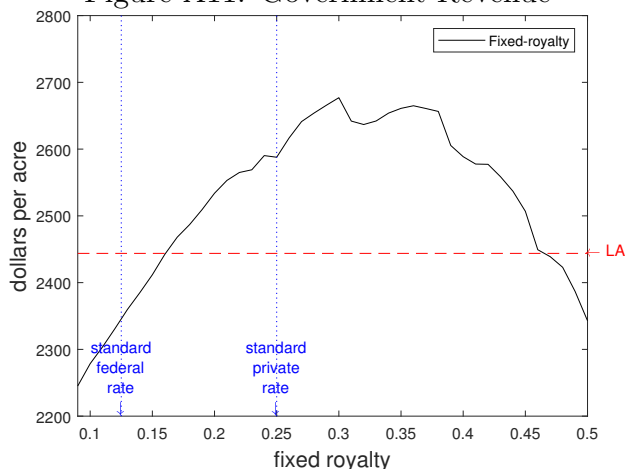
Notes: Solid line displays ex ante expected royalty revenue from counterfactual simulations of fixed-royalty auctions, as a function of the fixed royalty rate displayed on the x -axis. For comparison, the dashed horizontal line marks ex ante expected royalty revenue from observed bids in the Louisiana cash-royalty auction, and the vertical dotted line marks the average observed royalty rate resulting from that auction, 23%.

Figure A10: Cash Payment Revenue



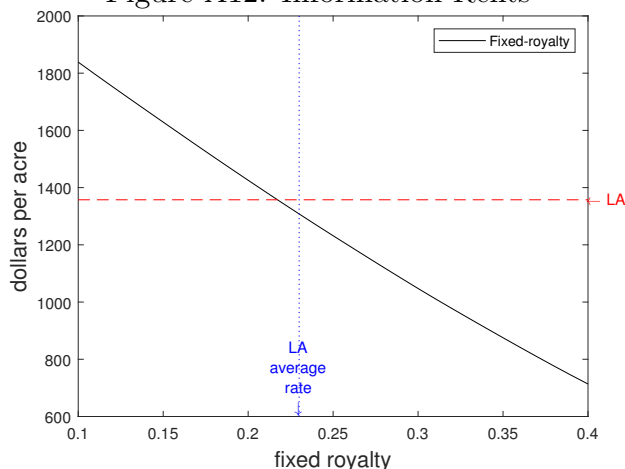
Notes: Solid line displays expected cash revenue from counterfactual simulations of fixed-royalty auctions, as a function of the fixed royalty rate displayed on the x -axis. For comparison, the dashed horizontal line marks cash revenue from observed bids in the Louisiana cash-royalty auction, and the vertical dotted line marks the average observed royalty rate resulting from that auction, 23%.

Figure A11: Government Revenue



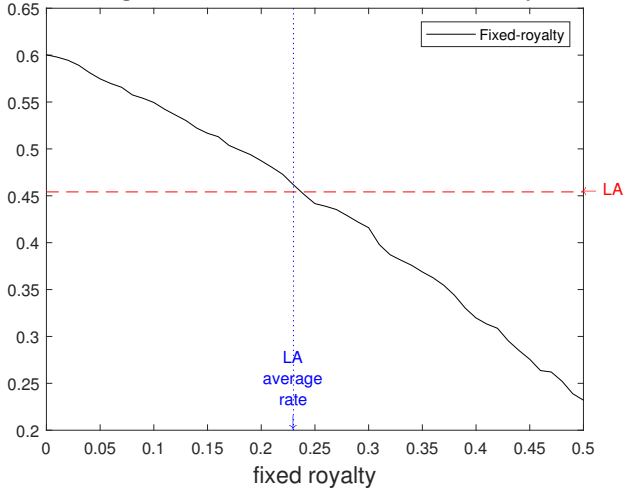
Notes: Solid line displays ex ante expected total government revenue, which is the sum of cash and royalties, from counterfactual simulations of fixed-royalty auctions, as a function of the fixed royalty rate displayed on the x -axis. For comparison, the dashed horizontal line marks ex ante expected total government revenue from observed bids in the Louisiana cash-royalty auction. For reference, vertical dotted lines mark the standard royalty rate on federal leases, 12.5%, and the prevalent royalty rate on privately held lands, 25%.

Figure A12: Information Rents



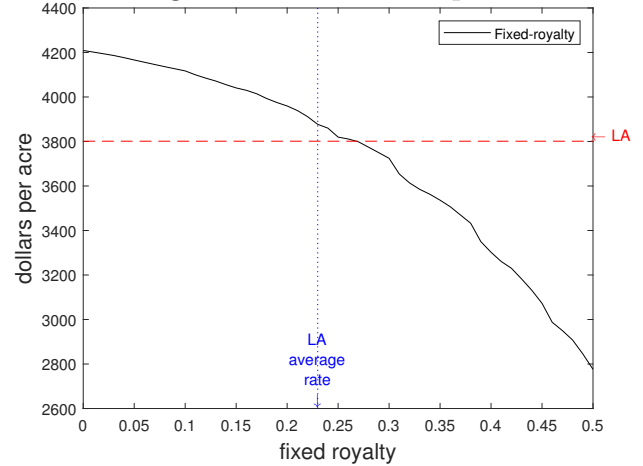
Notes: Solid line displays winning bidders' information rents from counterfactual simulations of fixed-royalty auctions, as a function of the fixed royalty rate displayed on the x -axis. For comparison, the dashed horizontal line marks information rents computed from observed bids in the Louisiana cash-royalty auction, and the vertical dotted line marks the average observed royalty rate resulting from that auction, 23%.

Figure A13: Exercise Probability



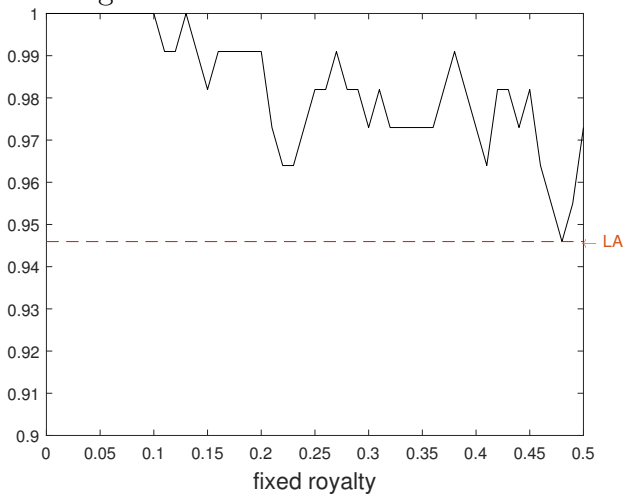
Notes: Solid line displays ex ante expected probability of lease development in counterfactual simulations of fixed-royalty auctions, as a function of the fixed royalty rate displayed on the x -axis. For comparison, the dashed horizontal line marks the analogous exercise probability computed from observed bids in the Louisiana cash-royalty auction, and the vertical dotted line marks the average observed royalty rate resulting from that auction, 23%.

Figure A14: Social Surplus



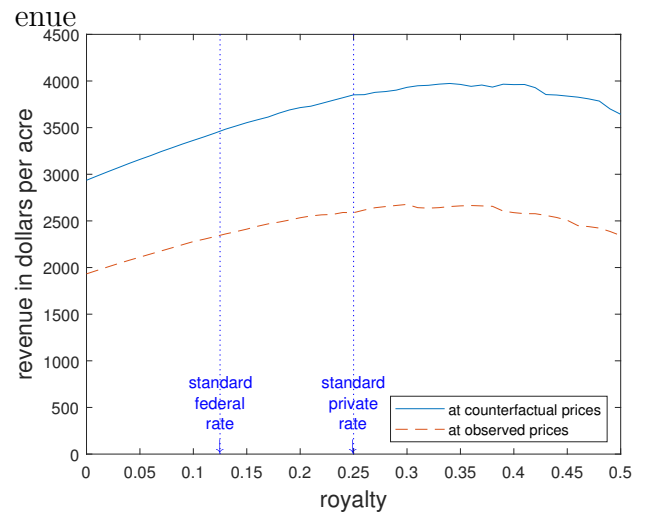
Notes: Solid line displays social surplus in counterfactual simulations of fixed-royalty auctions, as a function of the fixed royalty rate displayed on the x -axis. For comparison, the dashed horizontal line marks social surplus computed from observed bids in the Louisiana cash-royalty auction, and the vertical dotted line marks the average observed royalty rate resulting from that auction, 23%.

Figure A15: Allocative Performance



Notes: The solid line displays the proportion of fixed-royalty auctions that allocate the lease to the ex ante revenue-maximizing bidder according to counterfactual simulations, as a function of the fixed royalty rate displayed on the x -axis. For comparison, the dashed horizontal line marks the analogous proportion in the Louisiana cash-royalty auction.

Figure A16: Oil Price and Government Revenue



Notes: Figure displays ex ante expected total government revenue in counterfactual simulations of fixed-royalty auctions, as a function of the fixed royalty rate displayed on the x -axis. The solid line is at oil prices 20% higher than observed, while the dashed line is at observed oil prices.

References

- Black, Fischer.** 1976. “The Pricing of Commodity Contracts.” *Journal of Financial Economics*, 3(1): 167–179.
- Hendricks, Kenneth, Robert Porter, and Bryan Boudreau.** 1987. “Information, Returns, and Bidding Behavior in Ocs Auctions: 1954-1969.” *The Journal of Industrial Economics*, 35(4): 517–542.
- Hull, John C.** 2017. *Options, Futures, and Other Derivatives*. . 10th ed., New York:Pearson.
- Kellogg, Ryan.** 2014. “The Effect of Uncertainty on Investment: Evidence from Texas Oil Drilling.” *American Economic Review*, 104(6): 1698–1734.
- Kong, Yunmi.** 2020. “Not Knowing the Competition: Evidence and Implications for Auction Design.” *The RAND Journal of Economics*, 51(3): 840–867.
- Kong, Yunmi.** 2021. “Sequential Auctions with Synergy and Affiliation across Auctions.” *Journal of Political Economy*, 129(1): 148–181.
- Krasnokutskaya, Elena.** 2011. “Identification and Estimation of Auction Models with Unobserved Heterogeneity.” *The Review of Economic Studies*, 78(1): 293–327.
- Perrigne, Isabelle, and Quang Vuong.** 2021. “Econometric Methods for Auctions.” In . Vol. 7 of *Handbook of Econometrics*, , ed. Steven Durlauf, Lars Peter Hansen, James J. Heckman and Rosa Matzkin. Forthcoming.
- Quandl.** 1983-2019. “Historical Crude Oil Futures Prices, Wiki Continuous Futures, Daily.” Nasdaq Data Link, <https://data.nasdaq.com> (accessed April 2019).
- Sampford, Michael R.** 1953. “Some Inequalities on Mill’s Ratio and Related Functions.” *The Annals of Mathematical Statistics*, 24(1): 130–132.
- Takahashi, Hidenori.** 2018. “Strategic Design under Uncertain Evaluations: Structural Analysis of Design-Build Auctions.” *The RAND Journal of Economics*, 49(3): 594–618.
- Yoganarasimhan, Hema.** 2016. “Estimation of Beauty Contest Auctions.” *Marketing Science*, 35(1): 27–54.